A wavelength criterion for the validity of the Energy Finite Element Method for plates

I. Moens, D. Vandepitte and P. Sas
Department of Mechanical Engineering, division PMA, K.U.Leuven, Belgium
e-mail : ilse.moens@mech.kuleuven.ac.be

Abstract
This paper presents a fundamental study of the validity of the Energy Finite Element Method (EFEM) for plates with hysteresis damping. Assumptions and approximations in the derivation of the fundamental energy equations of EFEM limit the validity region of the method. Recent publications present indicators for limits of the validity region, based on experimental deduction and experience. This paper discusses a more fundamental explanation of the validity limits in terms of the assumptions and approximations of EFEM. For plates with hysteresis damping, a limit is found in terms of characteristic dimensions of the plate with respect to the wavelength. Plates with different shapes and boundary conditions are studied. Numerical examples with validation in analytic modal superposition solutions and classical dynamic FEM support the conclusions.

1. Introduction

At high frequencies, Statistical Energy Analysis (SEA) [1-3] represents a widely accepted, theoretical framework for the analysis of the dynamic response of complex systems. SEA uses kinetic energy as a general response descriptor. Complex vibro-acoustic systems are modelled as a composition of subsystems of similar modes. SEA parameters describe the ability of subsystems to store energy (modal density), to dissipate energy (internal loss factor) and to transfer energy (coupling loss factors). SEA provides information about the lumped energy stored in each subsystem.

The Energy Finite Element Method (EFEM) [4-11] is a more recent tool for the prediction of the vibrational behaviour of structures in the high frequency range. Like SEA, EFEM predicts mechanical energy based on energy equilibrium equations but where SEA uses macro subsystems, EFEM uses infinitesimal structural or acoustic subsystems. As a result, EFEM is capable of predicting the smoothed spatial variation of the mechanical energy and the application of local effects such as localised power inputs and local damping treatments is more straightforward. As shown in [5-7], the smoothed energy of EFEM in components like beams, plates or acoustic volumes is conceptually similar to the equations of static heat flow, which can easily be solved by the finite element method. Because of the finite element formulation of EFEM, a low-frequency classical FEM database can be used for a high-frequency EFEM calculation. This is a big advantage over SEA since SEA needs *(i)* a not-straightforward process of dividing a complex system into SEA subsystems and *(ii)* the derivation of a completely different database with SEA parameters.

Although the number of publications on applications of EFEM is growing, only few theoretical considerations can be found on the validity, accuracy and robustness of this predictive tool. Recent publications on EFEM [8-11] show some practical applications in which EFEM is successfully applied and experimentally validated for beam assemblies, sound transmission problems, a heavy equipment cab and marine applications. Based on experiments, Gur [8] expresses a wavelength criterion for beams and plates in order to get a lower limit of the frequency for the validity of EFEM. Vlahopoulos [10] expresses a more vague wavelength criterion, for deciding whether a component exhibits high frequency behaviour. A member is long (or exhibits high frequency behaviour) if there is uncertainty when comparing the exact dimension of a member with the number of waves within it.

In [4] the validity of EFEM was studied for single and coupled *square* plates. The validity limits of EFEM were compared to criteria that were found in literature for SEA and for experimental EFEM case studies. This paper extends the conclusions in [4] to plates of different shapes.

2. Theoretical background

This section gives a brief overview of the formulation of EFEM for flexural waves in plates. A steady-state energy balance of an infinitesimal part of a plate results in :

$$P_{in} = P_{diss} + \nabla \vec{I} \tag{1}$$

where P_{in} is the applied power ($[W/m^2]$), $\vec{I}$ is the intensity (or energy flow) vector ($[W/m]$) and P_{diss} is the dissipated power ($[W/m^2]$). The two right hand terms are expressed in terms of energy density e ($[J/m^2]$) in the next paragraphs.

2.1 Dissipation of energy due to internal hysteresis damping

Dissipation of energy can be caused by a large number of mechanisms. The present study adopts a hysteresis damping model. The structure's ability to dissipate energy is quantified by the material damping loss factor η. This factor appears in the complex elastic modulus $E_c = E(1 + j\eta)$ and the complex shear modulus $G_c = G(1 + j\eta)$.

According to [16], the time averaged dissipated power in a differential volume is proportional to the time averaged potential energy density :

$$\langle P_{diss} \rangle = 2\omega\eta \langle e_{pot} \rangle \tag{2}$$

where ω is the pulsation, η damping loss factor and '$\langle\rangle$' denotes a time averaged quantity.

If the time averaged potential energy density approximately equals the time averaged kinetic energy density, $\langle e_{pot} \rangle \cong \langle e_{kin} \rangle$, this equation becomes :

$$\langle P_{diss} \rangle = \omega\eta \langle e \rangle \tag{3}$$

with $\langle e \rangle$ the total time averaged energy density, sum of potential and kinetic time averaged energy, or twice the time averaged kinetic energy.

This is completely similar to the expression for energy dissipation within a SEA subsystem i :

$$P_{diss_i} = \omega\eta_i E \tag{4}$$

where η_i is the internal loss factor, P_{diss_i} ($[W]$) is the dissipated power in subsystem i and E ($[J]$) is the lumped energy of the subsystem (calculated as twice the kinetic energy).

The main approximation in this result, is the assumption that **the potential energy equals the kinetic energy**. In [6] it was observed that for finite *rods*, this assumption is acceptable in the high frequency range and when the energy quantities are frequency averaged. By frequency averaging the behaviour of finite structures tends towards the behaviour of infinite or semi-infinite structures. It was also observed that the potential and kinetic energies of higher damped structures are approximately equal at lower frequencies than less damped structures. When the quantities are frequency averaged, this difference between structures with different damping values diminishes.

This is a first and fundamental assumption that will provide limits on the validity region of energy methods with hysteresis damping. The hysteresis damping model is often applied when comparison is made between the high frequency energy methods and numerical classical dynamic FEM results, since damping is most easily included in classical FEM by means of a complex elasticity modulus.

2.2 Energy flow within plates

This paragraph develops the governing differential equation which relates the intensity or the energy flow with the energy density. The basic form of the *farfield* transverse displacement w of a plate due to a harmonic load with pulsation ω can be expressed as :

$$w = [A_x e^{-jk_x x} + B_x e^{jk_x x}][A_y e^{-jk_y y} + B_y e^{jk_y y}]e^{j\omega t} \tag{5}$$

where k_x and k_y are the complex wavenumbers in x and y direction at ω and A_x, B_x, A_y and B_y are complex coefficients depending on the boundary conditions. These coefficients describe the amplitudes of the *propagating* plane waves in the positive and negative x and y directions, respectively.

The time averaged total energy density e is :

$$\begin{aligned}
\langle e \rangle &= \langle e_{pot} \rangle + \langle e_{kin} \rangle \qquad (6)\\
&= \frac{h}{12E}\left(|\sigma_x|^2 + |\sigma_y|^2 - 2\nu\Re\left\{\sigma_x\sigma_y^*\right\} \dots \right.\\
&\quad \left. +2(1+\nu)\,|\tau_{xy}|^2 \right) + \frac{\rho h}{4}\left|\frac{\partial w}{\partial t}\right|^2\\
&= \frac{D}{4}\left(\left|\frac{\partial^2 w}{\partial x^2}\right|^2 + \left|\frac{\partial^2 w}{\partial y^2}\right|^2 + \dots \right.\\
&\quad 2\nu\Re\left\{(1+i\eta)\frac{\partial^2 w}{\partial x^2}\frac{\partial^2 w^*}{\partial y^2}\right\} + \dots\\
&\quad \left. 2\nu(1-\nu)\left|\frac{\partial^2 w}{\partial x \partial y}\right|^2 \right) + \frac{\rho h}{4}\left|\frac{\partial w}{\partial t}\right|^2
\end{aligned}$$

where the stresses σ_x, σ_y and τ_{xy} are the normal and shear stresses at the outer fibre (plane stress), h is the thickness of the plate, $D = Eh^3/[12(1-\nu^2)]$ is the bending stiffness of the plate, η is the damping loss factor as in paragraph 2.1, ν is the Poisson's ratio, ρ is the volumetric mass density and $\Re$ denotes the real part of a complex number.

The time averaged intensity in x and y direction can also be written in terms of the *farfield* displacement w :

$$\langle I_x \rangle = \frac{1}{2}\Re\left\{ D_c \left(\frac{\partial}{\partial x}\nabla^2 w \frac{\partial^2 w^*}{\partial t^2} - \ldots \right.\right. \tag{7}$$
$$\left.\left. \left[\frac{\partial^2 w}{\partial x^2} + \nu\frac{\partial^2 w}{\partial y^2}\right]\frac{\partial^2 w^*}{\partial x \partial t} - (1-\nu)\frac{\partial^2 w}{\partial x \partial y}\frac{\partial^2 w^*}{\partial y \partial t}\right)\right\}$$

$$\langle I_y \rangle = \frac{1}{2}\Re\left\{ D_c \left(\frac{\partial}{\partial y}\nabla^2 w \frac{\partial w^*}{\partial t} - \ldots \right.\right. \tag{8}$$
$$\left.\left. \left[\frac{\partial^2 w}{\partial y^2} + \nu\frac{\partial^2 w}{\partial x^2}\right]\frac{\partial^2 w^*}{\partial y \partial t} - (1-\nu)\frac{\partial^2 w}{\partial y \partial x}\frac{\partial^2 w^*}{\partial x \partial t}\right)\right\}$$

where $D_c = D(1+j\eta)$ is the complex bending stiffness of the plate.

When averaged over one wavelength, the relationship between the time averaged intensity components $\langle \underline{I}_x \rangle$ and $\langle \underline{I}_y \rangle$ and the time averaged energy density $\langle \underline{e} \rangle$ is [5] :

$$\left\langle \vec{\underline{I}} \right\rangle = -\frac{c_g^2}{\eta\omega}\nabla \langle \underline{e} \rangle \tag{9}$$

where c_g is the group speed of the flexural waves at ω and '$\_$' denotes a spatial averaged quantity.

Substitution of equations (3) and (9) in equation (1), yields :

$$-\frac{c_g^2}{\eta\omega}\nabla^2 \langle \underline{e} \rangle + \eta\omega \langle \underline{e} \rangle = 0 \tag{10}$$

This equation constitutes the governing differential equation for EFEM. The equation is conceptually similar to the steady-state heat flow equation (with a conduction and a convection term) and can be solved by the finite element method.

The main approximations in the derivation of the energy flow equation are the following :

- In EFEM, **only farfield waves** (or propagating waves) are retained in the analysis. The EFEM only captures the energy associated with the reverberant field [10]. The energy associated with the evanescent waves is ignored. The application of EFEM is valid when *several* wavelengths are present within a component. This requirement is equivalent to the SEA criterion for high modal density. When several wavelengths are available, there will be a mixing of phases due to the multiple reflected waves and a reverberant field is generated. Note that this is a basic assumption for both SEA and EFEM. The following sections try to quantify this *wavelength criterion*.
- Only **plane waves** are included in the analysis.
- Not only time and frequency averaging but also **spatial averaging** is necessary for the derivation of the basic EFEM equations. In theory, this averaging needs to be done over at least one wavelength.

3. Validity of EFEM for plates

This section discusses the validity of EFEM for plates excited out-of-plane. The first paragraph discusses some parameters from literature that give an indication of the applicability of EFEM. In the next paragraph, these criteria are cross-checked with the basic assumptions in EFEM for plates.

3.1 Critical parameters for the validity of EFEM

Where SEA approaches high-frequency vibrations from a *modal* point of view, EFEM is based on a *wave* approach. This section illustrates that some parameters that give an indication of the validity of SEA can be related to the wave approach in EFEM. In literature, also some indications can be found for the validity of EFEM from experimental deduction or experience. Both will be briefly addressed here.

Fahy [3] states that the uncertainty of SEA predictions may be unacceptably high when the modal overlap factors of the uncoupled subsystems are much less than unity. For low modal overlap factors, the results for a single sample of a class of system may be quite unrepresentative for the ensemble-average values.

The modal overlap factor is defined as :

$$MOF = \eta n(\omega)\omega \tag{11}$$

where $n(\omega)$ is the modal density (in modes per rad/s).

In order to obtain an equivalent criterion for EFEM, the modal overlap factor is expressed in terms of wave characteristics. For flexural waves in plates, the modal density is [1]:

$$n(\omega) = \frac{kS}{2\pi c_g} = \frac{k^2 S}{4\pi\omega} = \frac{\pi S}{\omega\lambda^2} \qquad (12)$$

with k the real part of the flexural wavenumber at ω, S the area of the finite plate, c_g the group speed of flexural waves in the plate at ω and λ the corresponding wavelength of the flexural waves at ω.

Define a non-dimensional parameter l:

$$l = \frac{L}{\lambda} \qquad (13)$$

where λ is the flexural wavelength and L is the characteristic plate length which can be defined as the square root of the area of the plate ($\sqrt{S}$). The non-dimensional parameter l expresses the number of wavelengths that are captured in the plate. The parameter l will increase with frequency for a particular plate, since wavelengths decrease with frequency.

With (13), the modal overlap factor for flexural waves can then be written as :

$$MOF = \eta\left(\frac{\pi}{\omega} l^2\right)\omega = \eta\pi l^2 \qquad (14)$$

and the criterion of Fahy [3], $MOF > 1$, becomes :

$$\eta\pi l^2 > 1 \quad \text{or} \quad l > \sqrt{\frac{1}{\pi\eta}} \qquad (15)$$

This extension of the criterion for SEA to EFEM implies that the lower limit of the frequency range where EFEM can be applied is dependent on the damping η.

Another criterion for the validity of EFEM can be found in [8]. Gur deduces out of experimental case studies a wavelength criterion for the validity of EFEM for plate structures. Gur uses a non-dimensional parameter with a slightly different definition : the *minimal* plate dimension over the largest wavelength of interest. If this non-dimensional parameter is larger than 2.43, EFEM can be used to analyse plate structures. In [8], no theoretical explanation of this number is given. In the next paragraphs the different options for the definition of a *characteristic* dimension of the plate are compared.

This requirement for EFEM is equivalent to the SEA criterion for high modal density. Fahy [3] states that it is necessary to have at least 5 resonant coupled modes in the frequency band of interest. For a single plate, the number of modes N in a frequency band can also be related to the non-dimensional parameter l, which results after some calculation in : (with (12))

$$\begin{aligned} N &= \int_{\omega_1}^{\omega_2} n(\omega)d\omega = \int_{\omega_1}^{\omega_2} \frac{\pi S}{\omega\lambda^2} d\omega \\ &= \pi S\left(\frac{1}{\lambda_1^2} - \frac{1}{\lambda_2^2}\right) = \pi\left(l_1^2 - l_2^2\right) \end{aligned} \qquad (16)$$

where λ_1 and λ_2 are the wavelengths at the lower frequency ω_1 and the higher frequency limit ω_2, and similar notations for the wavelength parameter l.

By using one-third octave frequency bands for the frequency averaging, the number of modes can be related to the non-dimensional parameter l at the lower frequency ω_1 :

$$N = \pi l_1^2\left(\sqrt[3]{2} - 1\right) \cong 0.82\, l_1^2 \qquad (17)$$

The criterion of Fahy [3], $N > 5$, becomes :

$$\pi l_1^2\left(\sqrt[3]{2} - 1\right) > 5 \quad \text{or} \quad l_1 > \sqrt{\frac{5}{\pi\left(\sqrt[3]{2} - 1\right)}} \cong 2.47 \qquad (18)$$

This number is very close to the experimentally deduced number by Gur [8] as described above. The next paragraphs validate the above *wavelength criteria* for the limits of the validity region of EFEM based on the assumptions in the derivation of EFEM.

3.2 Validity of EFEM on plates

As stated before, the basic equations of EFEM and SEA for the internal dissipation of energy due to hysteresis damping are completely similar (see section 2.1). Since EFEM calculates the spatial distribution of energy densities, the total energy balance of a *single* plate can be written as :

$$P_{in} = P_{diss} = \int_{S_{plate}} \eta\omega e \, dS \qquad (19)$$

Note that this basic equation is automatically fulfilled in SEA and EFEM. But, in theory, the energy ($\int_{S_{plate}} e dS$) that is calculated from the input power by equation (19) is equal to twice the potential energy where it is most commonly interpreted as the total energy or twice the kinetic energy. The remainder of this section investigates when the kinetic energy equals the potential energy for finite plates.

Property	Symbol	Value
elasticity modulus	E	$200GPa$
Poisson's coefficient	ν	0.3
mass density	ρ	$7800kg/m^3$
thickness	h	$3mm$

Table 1: Common properties of the plates.

An extensive study is performed on plates of different shapes with uniform hysteresis damping. Reference [4] discusses results for square plates. In this paper, rectangular plates with different aspect ratios and trapezoidal plates are studied. The plates are excited by a harmonic point force (out-of-plane) near the centre. Different boundary conditions (free-free and simply supported) were applied. This study aims at finding the most suitable descriptor of the *characteristic* length of the plate in the wavelength criterion : the *minimal* dimension (shortest distance between two non adjacent edges, as proposed by Gur [8]) or an *mean* dimension (square root of the surface area, as proposed in the previous section).

The displacement solution of a simply supported rectangular plate can be obtained by truncation of an infinite series (superposition of modes). The complete set of formulas can be found in [4]. For more general shapes (like in this paper the trapezoidal plates), displacement and stress results are obtained by a classical FEM calculation (with MSC Nastran) with a very fine mesh. The time averaged energy is calculated as in equation (6) and inserted in equation (19) to calculate the total dissipated power. Out of the displacement results, the time averaged input power is calculated as :

$$P_{in} = \frac{1}{2}\Re\left\{F\left(\frac{\partial w_l}{\partial t}\right)^*\right\} \qquad (20)$$

where w_l is the displacement at the excitation point. This input power is compared to the calculated dissipated power. The material and geometrical parameters of the plate that remain constant during the numerical tests are summarized in table 1.

For **rectangular** plates, numerous tests were performed with different plate dimensions, different damping loss factors (η ranging from 0.001 to 0.2), different frequencies and different aspect ratios (longest over shortest plate dimension): 1, $\pi/2$, 2 and 5. The plates were tested with simply supported boundary conditions. Similar as in [4], it was observed that the equality of the kinetic and potential energy was *not* dependent on the damping loss factors. However, different curves were obtained for plates with different aspect ratios. For a given aspect ratio, the difference between kinetic and potential energy seemed to be a unique function of the wavelength parameter l, as defined above. In other words, for each combination of plate dimensions with frequency that yields the same value for the wavelength parameter l, the same ratio of input power over dissipated power was obtained, when the dissipated power was calculated with the total energy density. When twice the potential energy was used to calculate the dissipated power, the dissipated power equals the input power as expected. This was used as a check of the numerical results.

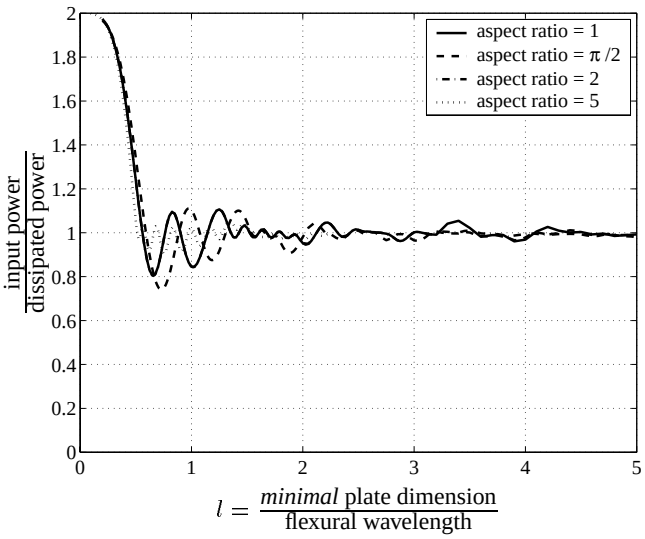

Figure 1: Rectangular plates with different aspect ratios, input power over total dissipated power.

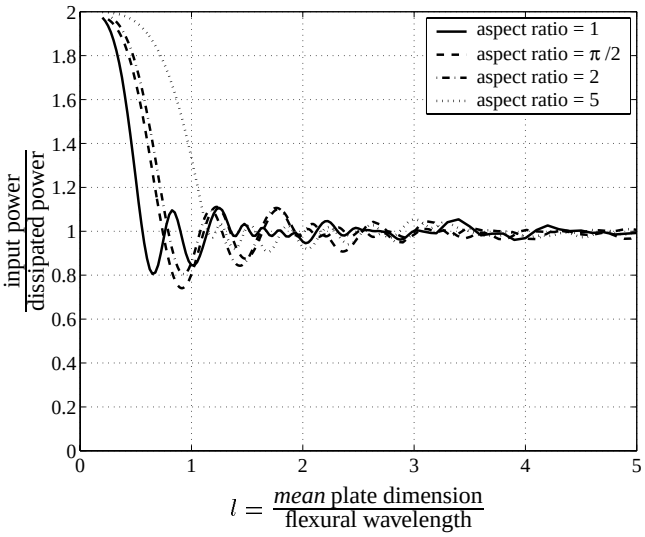

Figure 2: Rectangular plates with different aspect ratios, input power over total dissipated power.

Figures 1 and 2 show the input power compared to the total dissipated power for simply supported rectangular plates with aspect ratios equal to 1 (square plate), $\pi/2$, 2 and 5. The different suggestions for the definition of the wavelength parameter (as mentioned before) are shown. Figure 1 uses the *minimal* dimension as the characteristic plate dimension, i.e. $l = L_{min}/\lambda$ with L_{min} the minimal plate dimension and λ the flexural wavelength. Figure 2 uses the *square root of the surface area* as characteristic length, i.e. $l = L_{mean}/\lambda$ with $L_{mean} = \sqrt{S}$ where S is the area of the plate. Note that the difference between both definitions is a factor equal to the square root of the aspect ratio.

Comparison of figures 1 and 2 confirm the expected result that the *minimal* plate dimension is a more relevant parameter than the *mean* plate dimension in the wavelength criterion. The same conclusion can be obtained for more general **trapezoidal shaped** plates. Two different trapezoidal plates were studied as shown in figures 3 and 4. For the trapezoidal plate in figure 3, the minimal plate dimension is $0.6m$, where the *mean* plate dimension (defined as the square root of the surface area) is equal to $\sqrt{0.9m^2} \cong 0.95m$. For the trapezoidal plate in 4, the minimal plate dimension is $0.4m$ (note that this does *not* correspond to the shortest edge), where the *mean* plate dimension is equal to $0.6m$.

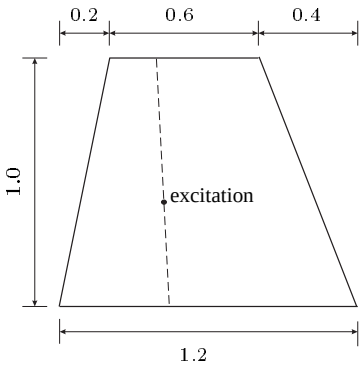

Figure 3: Trapezoidal plate, shape 1 (dimensions in $[m]$).

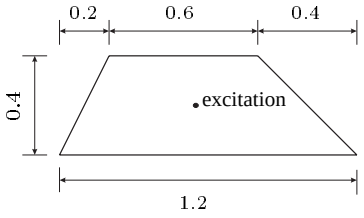

Figure 4: Trapezoidal plate, shape 2 (dimensions in $[m]$).

The trapezoidal plates as described above, are subjected to 2 different boundary condition sets : simply supported edges and free-free conditions. Numerical results for the displacements (to calculate the kinetic energy, as in (6)) and the stresses (to calculate the potential energy, as in (6)) were obtained by a classical dynamic finite element calculation with a very fine mesh : more than 8 elements per half wavelength. The material properties and the thickness are again as in table 1. Results for both trapezoidal plates for both boundary condition sets are shown in figure 5 (with the *minimal* dimension as characteristic plate dimension in the wavelength criterion) and figure 6 (with the *mean* dimension in the wavelength criterion).

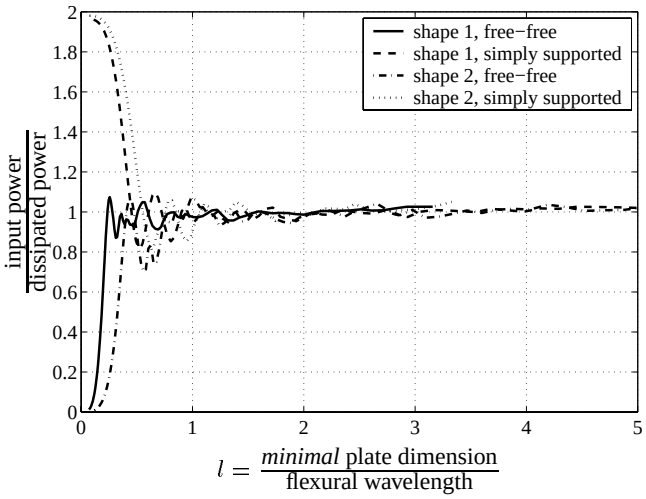

Figure 5: Trapezoidal plates (shapes as in figures 3 and 4), with 2 different boundary condition sets.

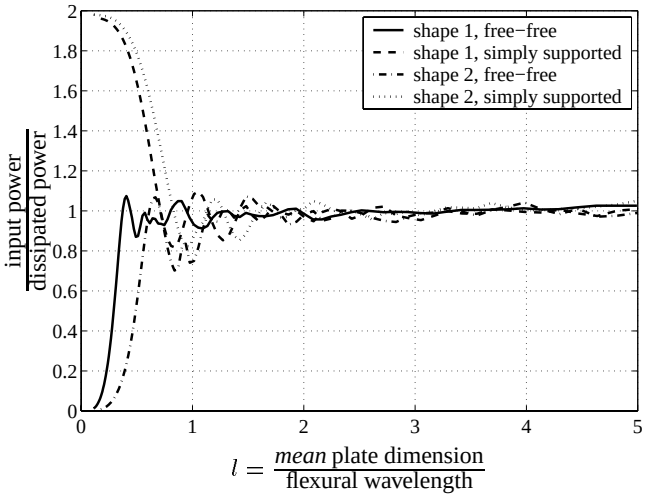

Figure 6: Trapezoidal plates (shapes as in figures 3 and 4), with 2 different boundary condition sets.

The results in figures 1, 2, 5 and 6 suggest that a *wavelength criterion* as defined in the previous paragraph can be explained in the use of kinetic or total energy in the equations for damping losses instead of potential energy. For high values of the parameter l, the kinetic and potential energy can be assumed to be equal, whereas at low values the differences can be very large. The use of the *wavelength criterion* with the *minimal* plate dimension is better than the criterion with the *mean* plate dimension.

The prediction of the **spatial distribution of the energy density** is a major advantage of EFEM over SEA. As stated before, EFEM predicts a smoothed approximation of the energy density. Typical examples of the smoothed spatial distribution of the energy density in a single rectangular plate are reported in [5]. Figures 7 and 8 present typical results of the spatial distribution of the energy density in the trapezoidal plate as in figure 3 along the dashed line. In figure 7, the damping loss factor η is 0.2, where in figure 8 the damping loss factor η is equal to 0.01. The results are shown for the one-third frequency band of $2000Hz$. In both figures, the smoothed trend of the energy density is captured, with an underestimation near the excitation and an overestimation farther away from the excitation. By comparing the two figures, it is clear that in structures with higher damping, the results from the classical FEM are closer to the EFEM predictions since the local variations of the energy density become smaller. A similar conclusion holds when comparing results at different frequencies : there is a better match at higher frequencies. In structures with low damping values and at lower frequencies, the EFEM solution provides only a mean value, similar as in SEA. These observations confirm the criterion in equation (15) qualitatively.

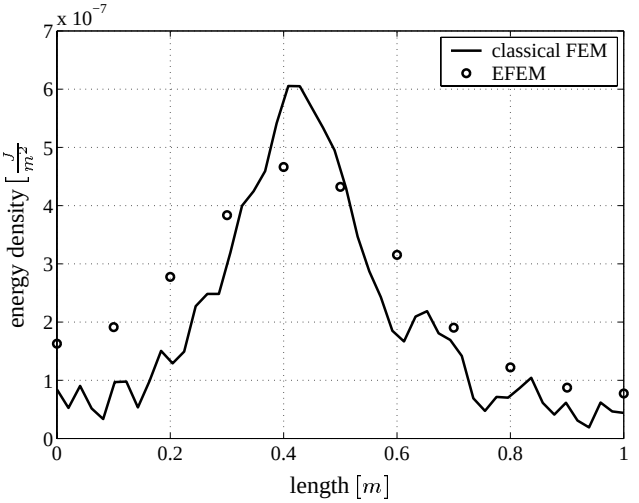

Figure 7: Energy density along the dashed line in figure 3, for $\eta = 0.2$, at $2000Hz$, comparison between classical FEM and EFEM results.

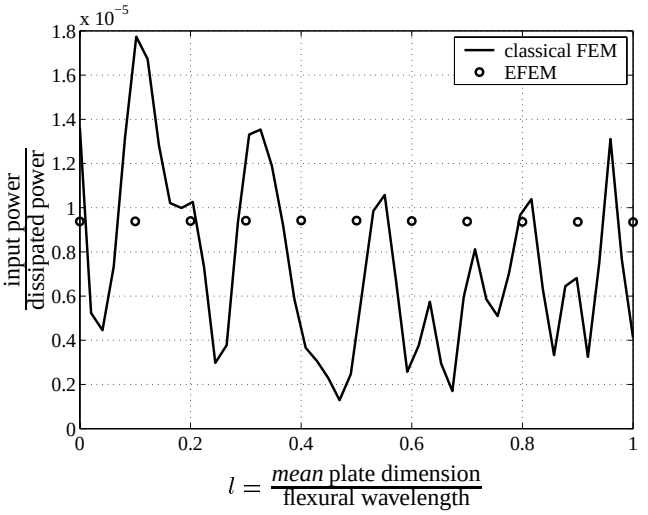

Figure 8: Energy density along the dashed line in figure 3, for $\eta = 0.01$, at $2000Hz$, comparison between classical FEM and EFEM results.

4. Conclusions

This paper discusses the validity of EFEM for plates of different shapes with uniform hysteresis damping. *Modal* criteria for the applicability of SEA from literature are expressed in terms of the *wave* characteristics for EFEM. In literature, also experimentally deduced wavelength criteria are reported. This paper links these *wavelength criteria* with the basic assumptions of EFEM. The equality of kinetic and potential mechanical energy is found to be equivalent to the *wavelength criterion* that the characteristic plate dimension must be higher than 2.4 times the shortest wavelength in the frequency range of interest. Below this value, the total energy equilibrium (input power equals total dissipated power) does not hold. This paper suggests an optimal choice for the *characteristic* plate dimension as the *minimal* plate dimension. The spatial variation of the energy density within the plates is a better approximation for the reference solution at higher frequencies (shorter wavelengths) and for structures with higher damping.

References

1. R.H. Lyon and R.G. DeJong, *Theory and Application of Statistical Energy Analysis*, Butterworth-Heinemann, USA (1995).

2. K. De Langhe, *High Frequency Vibrations : Contributions to Experimental and Computational SEA Parameter Identification Techniques*, Ph.D. thesis, K.U.Leuven, Belgium (1996).

3. F.J. Fahy and A.D. Mohammed, *A study of uncertainty in applications of SEA to coupled beam and plate systems, part I : computational experiments*, Journal of Sound and Vibration, Vol. **158(1)**, pp.45-67, (1992).

4. I. Moens, D. Vandepitte and P. Sas, *Study of the applicability of EFEM for plates*, Proc. of the Novem conference, Lyon (2000).

5. O.M. Bouthier and R.J. Bernhard, *Simple models of the energetics of transversely vibrating plates*, Journal of Sound and Vibration, Vol. **182(1)**, 149-164 (1995).

6. P.E. Cho, *Energy Flow Analysis of Coupled Structures*, Ph.D. thesis, Purdue university, USA (1993).

7. F. Bitsie, *The structural-acoustic energy finite element method and energy boundary method*, Ph.D. thesis, Purdue university, USA (1996).

8. Y. Gur, D.A. Wagner and K.N. Morman, *Energy finite element analysis methods for mid-frequency NVH applications*, Proc. of the 1999 Noise and Vibration Conf. SAE, pp.1159-1167 (1999).

9. S. Wang and R.J. Bernhard, *Energy Finite Element Method (EFEM) and Statistical Energy Analysis (SEA) of a heavy equipment cab*, Proc. of the 1999 Noise and Vibration Conf. SAE, pp.443-450 (1999).

10. N. Vlahopoulos, L.O. Garza-Rios and C. Mollo, *Numerical Implementation, Validation and Marine Applications of Energy Finite Element Formulation*, Journal of Ship Research, Vol. **43(3)**, pp.143-156 (1999).

11. N. Vlahopoulos and X. Zhao, *Basic Development of Hybrid Finite Element Method for Midfrequency Structural Vibration*, AIAA Journal, Vol.**37(11)**, pp.1495-1505 (1999).

12. R.S. Langley and K.H. Heron, *Elastic wave transmission through plate/beam junctions*, Journal of Sound and Vibration, Vol.**143(2)**, pp.241-253 (1990).

13. L. Cremer, M. Heckl and E.E. Ungar, *Structure-Borne Sound*, Springer-Verlag, New York, USA (1988).